Bearing Load of Scroll Compressor for Automotive Air Conditioner

Takahisa Hirano[*1] **Yasuharu Maruiwa**[*2]
Kiyoshi Hagimoto[*3]

In order to achieve compact size, light weight, and reduce the machines cost, estimation of actual load acting on the parts is very important for the appropriate design. The cylinder pressure and crankshaft kinematics of refrigerating scroll compressor are usually simulated, but the accuracy of kinematic analysis of refrigerating compressor has not been verified because the compressor is small and the parts are under refrigerant pressure. We have analytically and experimentally studied the bearing load behavior of a scroll compressor for an automotive air conditioner. (1) A statically indeterminate kinematic model of the crankshaft system has been developed to improve the simulation accuracy. (2) Each load acting on the ball bearings under compressor operating has been measured. (3) The simulated and measured values of bearing loads agreed, and bearing load behavior of the scroll compressor has been clarified.

1. Introduction

In order to achieve compact size and light weight, it is important to accurately estimate the loads acting on parts and to design a machine correctly considering these loads. The loads acting on the parts of the refrigerating scroll compressor of an air conditioner are usually determined by analyzing the pressure in the compression pocket and the kinematics of the rotary shaft system. Therefore, it is very important to improve the accuracy of the kinematic analysis of the compressor and fully verify its appropriateness.

Compression pocket pressure analysis, parts kinematic analysis[(1)] and pressure and temperature measurement[(2)] have often been performed for the refrigerating scroll compressor of air conditioners, but the loads acting on the parts have rarely been measured[(3)]. One of the main parts of the compressor of an automotive air conditioner is the roller bearing. As to the measurement of the load acting on the roller bearing, though a report on the tapered roller bearing of a large machine used at ambient pressure is available[(4)], no such measurement report can be found for the refrigerating scroll compressor of an air conditioner because the compressor is small and the parts are exposed to refrigerant gas and lubricating oil mist at high pressure. In the present study, the following have been performed in relation to the bearing load of a scroll compressor for an automotive air conditioner.

(1) A statistically indeterminate kinematic model of the whole shaft system composed of the clutch bearing, main bearing, sub bearing and crank shaft has been developed to improve the accuracy of kinematic simulation.
(2) The load acting on the roller bearing with the compressor driven using refrigerant has been measured to verify the above-mentioned simulation and to clarify the characteristics of the bearing load.

2. Compressor

Fig. 1 shows the cross section of the scroll compressor for an automotive air conditioner. The scroll compressor is composed of a pair of scrolls. The orbiting scroll (180° phase-different from the fixed scroll) revolves (without rotating) around the fixed scroll[(5)]. As a result, an enclosed space is formed between the two scrolls, sucking refrigerant gas from the scroll circumference. As it sequentially moves inward, pressure buildup is caused owing to the decrease in volume. Finally, high pressure gas is discharged through the discharge port provided near the center of the fixed scroll. The crank shaft which drives the drive bearing of the orbiting scroll is supported by the main bearing and sub bearing and the other end is connected to the clutch. The crank shaft is driven through the clutch by the engine to compress the refrigerant gas.

Table 1 shows the dimensions of the scroll compressor for an automotive air conditioner analyzed and measured here.

3. Bearing load analysis

3.1 Kinematic model

In the previous kinematic analysis[(1)] of a scroll compressor, a model was used in which the crank shaft load is supported by

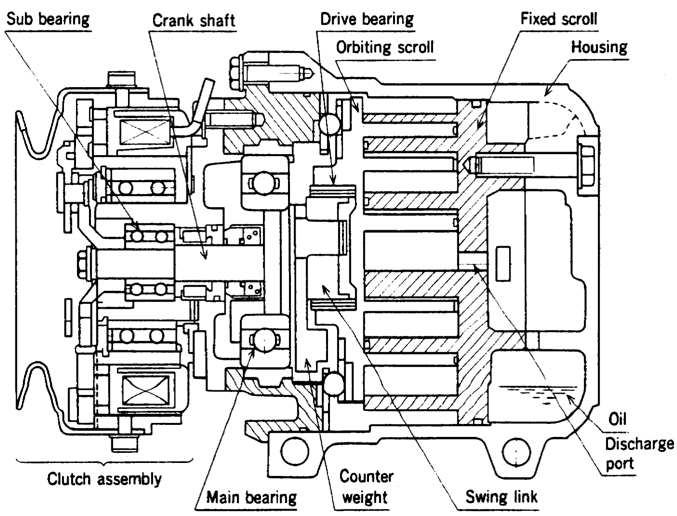

Fig. 1 Scroll compressor for automotive air conditioner
Cross section of compressor is shown.

Table 1 Dimensions of scroll compressor

Item		Dimension
Base circle radius	(mm)	3.0
Wrap thickness	(mm)	4.57
Wrap height	(mm)	33.6
Displacement	(cm^3/rev.)	78.8
Rotating speed	(min^{-1})	800 to 11 200
Refrigerant		CFC 12, HFC 134 a

*1 Air-Conditioning & Refrigeration Machinery Works
*2 Nagoya Research & Development Center, Technical Headquarters
*3 Churyou Engineering Co. Ltd.

the main bearing and sub bearing. However, in the case of the compressor for an automotive air conditioner shown in Fig. 1, the crank shaft is supported through the armature by the clutch bearing because the clutch is connected to the crank shaft. Therefore, we have made an analysis model considering the elastic deformation of the armature plate spring to develop a statistically indeterminate kinematic analysis model of the whole crank shaft system.

Fig. 2 shows the forces of the analyzed crank shaft system. The following have been assumed to develop the kinematic model.

(1) Elastic displacement of the armature plate spring and the bearing ball contact zone is caused. The elastic displacement of the armature plate spring due to longitudinal tension and compression is considered. For the elastic displacement of the bearing balls, changing of the loading ratio is considered.

(2) The radial gap between the sub bearing and main bearing is considered.

(3) The discrepancy between the centers of the sub bearing and main bearing is considered.

The kinematic model is based on the following basic equations. As the crank shaft and clutch can be considered to be one body, equations (1) and (2) are obtained by applying the three-dimensional kinematics to it.

Balance of forces:

$$-\boldsymbol{F}_P-\boldsymbol{F}_{st}+\boldsymbol{W}_G+\boldsymbol{F}_1+\boldsymbol{F}_2+\boldsymbol{F}_3 +\boldsymbol{F}_{B1}+\boldsymbol{F}_{B2}+\boldsymbol{F}_{CT}+\boldsymbol{F}_{BT1}+\boldsymbol{F}_{BT2}=0 \quad (1)$$

Balance of moments:

$$-\begin{pmatrix} r_{PB} \\ -l_{P1}\end{pmatrix}\times\begin{pmatrix}\gamma_{P1}\boldsymbol{F}_P\\0\end{pmatrix}-\begin{pmatrix} r_{PB} \\ -l_{P2}\end{pmatrix}\times\begin{pmatrix}\gamma_{P2}\boldsymbol{F}_P\\0\end{pmatrix}$$
$$-\begin{pmatrix}0\\ z_{st}-z_{P1}-l_{P1}\end{pmatrix}\times\begin{pmatrix}\boldsymbol{F}_{st}\\0\end{pmatrix}+\begin{pmatrix}0\\l_G\end{pmatrix}\times\begin{pmatrix}\boldsymbol{W}_G\\0\end{pmatrix}$$
$$+\begin{pmatrix}r_1\\-l_1\end{pmatrix}\times\begin{pmatrix}\boldsymbol{F}_1\\0\end{pmatrix}+\begin{pmatrix}r_2\\l_2\end{pmatrix}\times\begin{pmatrix}\boldsymbol{F}_2\\0\end{pmatrix}+\begin{pmatrix}r_3\\l_3\end{pmatrix}\times\begin{pmatrix}\boldsymbol{F}_3\\0\end{pmatrix}$$
$$+\begin{pmatrix}r_{B1}\\l_{B1}\end{pmatrix}\times\begin{pmatrix}\boldsymbol{F}_{B1}\\0\end{pmatrix}+\begin{pmatrix}r_{B2}\\l_{B2}\end{pmatrix}\times\begin{pmatrix}\boldsymbol{F}_{B2}\\0\end{pmatrix}+\begin{pmatrix}r_{CT}\\l_{CT}\end{pmatrix}\times\begin{pmatrix}\boldsymbol{F}_{CT}\\0\end{pmatrix}$$
$$+\begin{pmatrix}r_{BT1}\\l_E\end{pmatrix}\times\begin{pmatrix}\boldsymbol{F}_{BT1}\\0\end{pmatrix}+\begin{pmatrix}r_{BT2}\\l_E\end{pmatrix}\times\begin{pmatrix}\boldsymbol{F}_{BT2}\\0\end{pmatrix}=\begin{pmatrix}0\\0\end{pmatrix} \quad (2)$$

Then, elastic displacement occurs in the armature plate spring. The relation between the internal forces due to this displacement and the external forces is expressed as follows.

Balance of forces:

$$\Phi(\zeta)\begin{pmatrix}-x_A\Delta_{r1}\\0\end{pmatrix}+\Phi\left(\zeta+\frac{2}{3}\pi\right)\begin{pmatrix}-x_A\Delta_{r2}\\0\end{pmatrix}$$
$$+\Phi\left(\zeta+\frac{4}{3}\pi\right)\begin{pmatrix}-x_A\Delta_{r3}\\0\end{pmatrix}=\boldsymbol{F}_{CT}^*+\boldsymbol{F}_{BT1}^*+\boldsymbol{F}_{BT2}^* \quad (3)$$

Balance of moments:

$$r_{1*}\times\Phi(\zeta)\begin{pmatrix}-x_A\Delta_{r1}\\0\end{pmatrix}+r_{2*}\times\Phi\left(\zeta+\frac{2}{3}\pi\right)$$
$$\cdot\begin{pmatrix}-x_A\Delta_{r2}\\0\end{pmatrix}+r_{3*}\times\Phi\left(\zeta+\frac{4}{3}\pi\right)\begin{pmatrix}-x_A\Delta_{r3}\\0\end{pmatrix}$$
$$=\boldsymbol{r}_{CT}\times\boldsymbol{F}_{CT}+\boldsymbol{r}_{BT1}\times\boldsymbol{F}_{BT1}+\boldsymbol{r}_{BT2}\times\boldsymbol{F}_{BT2} \quad (4)$$

The following geometrical relation between the sub bearing and main bearing, and the elastic displacement of each bearing and armature plate spring is obtained.

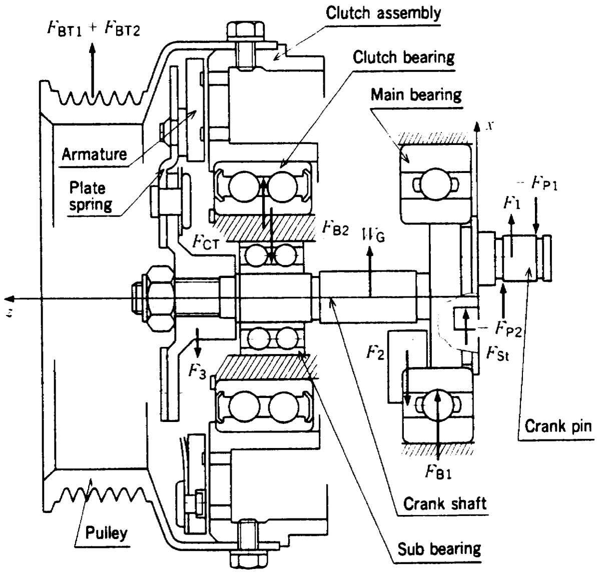

Fig. 2 Analysis model
Analysis model of bearing and clutch assembly is shown.

$$\Phi(\alpha_{B2})\begin{pmatrix}C_{B2}+\Delta_{B2}\\0\end{pmatrix}=\Phi(\alpha_{CT})\begin{pmatrix}-C_{CT}-\Delta_{CT}\\0\end{pmatrix}+\varphi(\theta)\,r_C+\begin{pmatrix}\xi\\\eta\end{pmatrix} \quad (5)$$

3.2 Solution

Because the crank shaft, of which the crank pin gas compression load, etc. are applied, is supported by three bearings, it is a statically indeterminate model considering elastic deformation. The main bearing always supports the load because of the compressor's construction. Therefore, kinematically, the following two cases are presumed.

Ⓐ The main, sub and clutch bearings support the load.

Ⓑ The sub or clutch bearing and the main bearing support the load.

On the assumption that there are two cases as shown below where the sub bearing meets the crank shaft and where it does not, all the equations have been solved.

(1) Case where the shaft does not meet the sub bearing

Sub bearing displacement d_{B2} is an unknown quantity. This displacement is determined by means of simulation calculation. If the solution indicates that the shaft does not meet the sub bearing, it gives solution (Ⓑ the main bearing and clutch bearing support the load). If the solution indicates that the shaft meets the sub bearing, proceed to the following case (2).

(2) Case where the shaft meets the sub bearing

In this case, while the main bearing and sub bearing meet the shaft, the clutch bearing may or may not meet the shaft. Using the calculation result of (1), solve the equations until sub bearing displacement d_{B2} equals sub bearing radial gap C_{B2}. If clutch bearing reaction force F_{CT} is positive at this point, the sub bearing and clutch bearing meet the shaft (Ⓐ the main, sub and clutch bearings support the load). If clutch bearing reaction force F_{CT} becomes 0 before this point, each value at that point is a solution (Ⓑ the main bearing and sub bearing support the load).

4. Measurement of cylinder pressure and bearing load

4.1 Measurement of cylinder pressure

There are two ways to determine the cylinder pressure change in the compression pocket causing the bearing load: measuring the cylinder pressure of an actual compressor and determining the cylinder pressure by means of analysis. We measured the cylinder pressure waveform and used it for the input condition of the shaft system kinematic analysis.

In the case of the scroll compressor, several compression pockets are formed at one time, sequentially moving inward along the scroll. Therefore, in order to measure the cylinder pressure waveform throughout the compression process, it is necessary to use several pressure sensors and combine their outputs[4]. **Fig. 3** shows an example of the cylinder pressure diagram into which the output waveforms of several pressure sensors are synthesized. From this, we obtained the cylinder pressure diagram of a pair of right and left compression pockets.

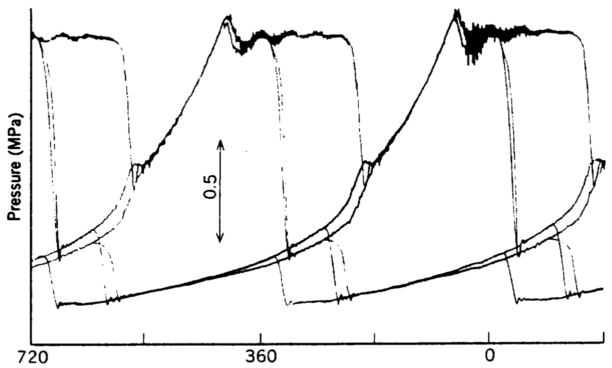

Fig. 3 Cylinder pressure diagram
Example of measurement of cylinder pressure changes is shown.

4.2 Measurement of bearing load

To measure the load acting on the ball bearing, we nicked the housing into which the outer race is forced, detected the deformation of the outer race with a strain gage, and then converted it into a load. **Table 2** shows the dimensions of the ball bearing being measured. Though a double angular ball bearing is used for the sub bearing of an actual compressor, it is replaced with a single ball bearing for the purpose of measurement. In order to increase the number of points for verifying the simulation accuracy, we measured the main bearing and sub bearing at six points each.

The load acting on the bearing of the scroll compressor is a rotational load whose direction changes with shaft rotation. The positions of the balls of the ball bearing also move with shaft rotation. As a result, as shown in **Fig. 4**, the strain gage indicates maximum output when the load direction, ball position and strain gage position are aligned; the output of the strain gage becomes small when they are not aligned. Therefore, when calibrating the strain gage, we obtained the maximum output of the strain gage by rotating the shaft while applying a load.

In measuring the load of an actual machine, as shown in **Fig. 5**, by superimposing many shaft rotation output waveforms of one strain gage, we obtained the envelope curve which was used to determine the load. For explanation purposes, Fig. 5 (b) shows an example in which only 12 waveforms are superimposed. In the actual measurement, however, we superimposed more than 120 waveforms to obtain the envelope curve.

Table 2 Dimension of ball bearing

Item		Main bearing	Sub bearing
Model		6207	6001
Bearing diameter	(mm)	72	28
Bearing width	(mm)	17	8
Ball number		9	8
Ball diameter	(mm)	11.112	4.763
Ball pitch	(deg.)	40	45

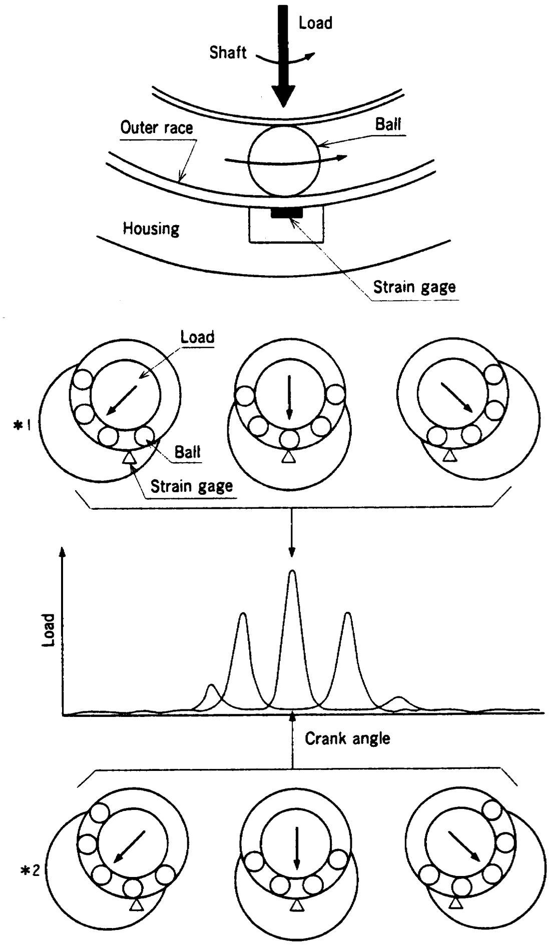

*1 Strain gage position, load direction and ball position are aligned.
*2 Ball position is not aligned.

Fig. 4 Bearing load measuring method
Ball bearing load measuring method is shown.

5. Results of simulation and measurement

The results of the bearing load simulation and measurement are shown in **Fig. 6**. The ratio of the main bearing-supported load to the sub bearing-supported load is 4 to 1 for both the simulation and measured values. The absolute value of main bearing load is slightly higher in case of the simulation. The load acting on the clutch bearing is nearly equal to the belt tension, which indicates that the main bearing and sub bearing

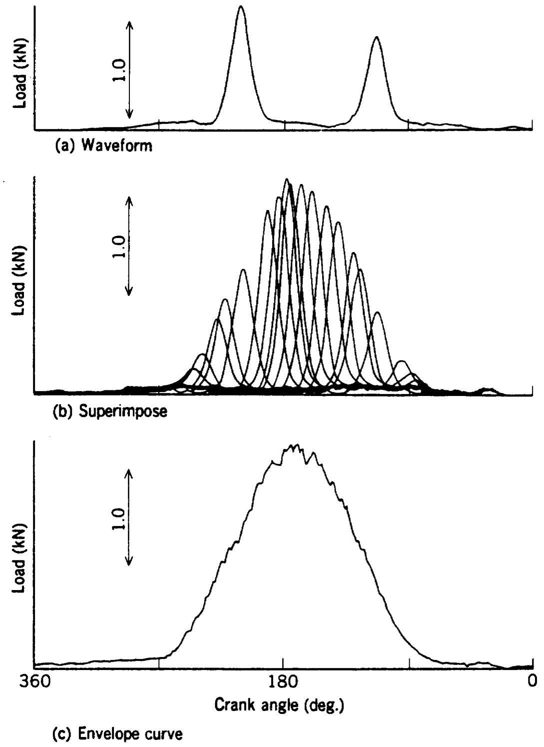

Fig. 5 Bearing load measurement
The envelope curve is obtained by superimposing output waveforms for one rotation and is used to determine the bearing load.

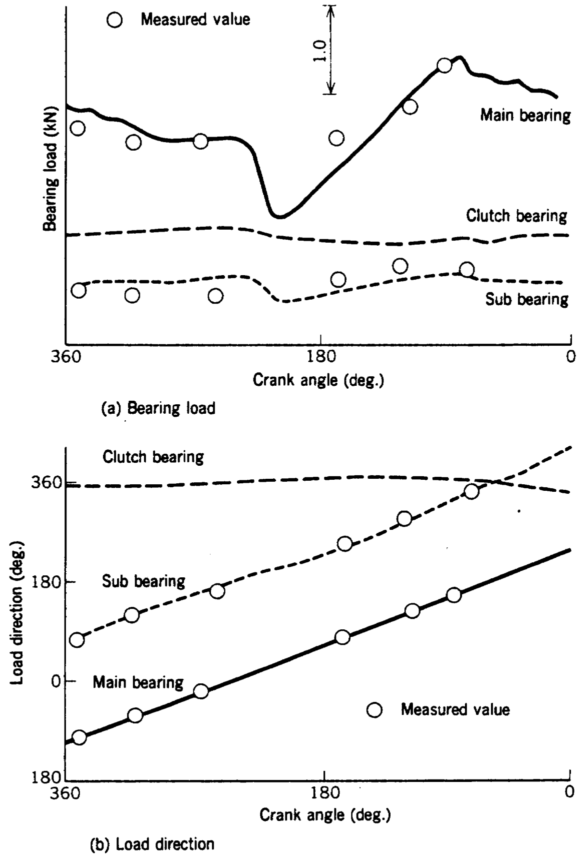

Fig. 6 Bearing load and load direction
The measured result and calculated result agree very well with each other. The main bearing load direction is about 110°—115° behind the crank angle and the sub bearing is 180° phase-different from the main bearing.

support the crank shaft load. In other words, the restraint of the clutch spring is relatively small in the present construction, so the clutch has little influence on the bearing system of the compressor. The problems to be solved concerning the simulation are as follows: estimating the out-of-plane deformation spring constant of the clutch plate spring when the force is transmitted in the rotating direction, and presuming the degree and direction of dislocation of the centers of the armature and crank shaft when the clutch armature is engaged.

The main bearing load direction is about 110°— 115° behind the orbiting scroll direction (crank angle direction) and the sub bearing is 180° phase-different from the main bearing. The clutch bearing load direction is constant regardless of the crank angle and is the same as the belt tension direction. The results of the simulation and measurement agree very well with each other regarding the main bearing and sub bearing load direction.

As shown above, the adequacy of the newly developed kinematic model of the whole shaft system including the clutch has been verified for both the load and its direction.

6. Conclusion

We have analytically and experimentally studied the bearing load of the scroll compressor for an automotive air conditioner in which the driving force is transmitted by means of the clutch. We have tried to improve the accuracy of the kinematic simulation of the scroll compressor and clarified the bearing load behavior. We have effectively utilize this simulation for the development of scroll compressors and will try to develop new technology meeting the needs of society.

Legend

F_{B1}, F_{B2} F_{CT}: reaction force from main bearing, sub bearing and clutch bearing
F_{BT1}, F_{BT2}: tension of belt tight side and slack side
F_P, F_{ST}: reaction force from crank pin and stopper
F_{P1}, F_{P2}: $\gamma_{21}F_2$, $\gamma_{P2}F_P$
F_1, F_2, F_3: centrifugal force of crank pin section, sub counter weight and armature
W_G: weight of crank shaft
Δ_{B2}, Δ_{CT}: Hertz deformation of sub bearing and clutch bearing
Δ_{r1}, Δ_{r2}, Δ_{r3}: longitudinal displacement of plate spring of armature
C_{B2}, C_{CT}: clearance of sub bearing and clutch bearing
d_{B2}: displacement of sub bearing
ξ, η: displacement of armature plate
ζ: direction angle of plate spring of armature
α_{B1}, α_{B2}, α_{CT}: direction angle of F_{B1}, F_{B2}, F_{CT}
χ_A: longitudinal elastic coefficient of plate spring of armature
r_C: vector from center of clutch to center of sub bearing
r_{B1}, r_{B2}, r_{CT}, r_{BT1}, r_{BT2}, r_{PB}, r_1, r_2, r_3
: vector on plane at right angles to axis from center of crank shaft to action center of F_{B1}, F_{B2}, F_{CT}, F_{BT1}, F_{BT2}, F_P, F_1, F_2 and F_3

$\boldsymbol{F}_{CT}{}^*$, $\boldsymbol{F}_{BT1}{}^*$, $\boldsymbol{F}_{BT2}{}^*$
: $\boldsymbol{F}_{CT}$, $\boldsymbol{F}_{BT1}$ and $\boldsymbol{F}_{BT2}$ whose direction is changed by a certain angle

$\boldsymbol{r}_1{}^*$, $\boldsymbol{r}_2{}^*$, $\boldsymbol{r}_3{}^*$: position vector at three points on the plate spring of armature

γ_{P1}, γ_{P2}: distribution coefficient of $\boldsymbol{F}_P$ to axial l_{P1} and l_{P2}

z_{ST}, z_{P1}: axial distance from fixed scroll chip to position where $\boldsymbol{F}_{ST}$, $\gamma_{P1}\boldsymbol{F}_P$ act

l_G, l_{P1}, l_{P2}, l_{B1}, l_{B2}, l_{CT}, l_E, l_1, l_2, l_3
: axial distance from crank pin base to $\boldsymbol{W}_G$, $\gamma_{P1}\boldsymbol{F}_P$, $\gamma_{P2}\boldsymbol{F}_P$, $\boldsymbol{F}_{B1}$, $\boldsymbol{F}_{B2}$, $\boldsymbol{F}_{CT}$, $\boldsymbol{F}_{BT1}$, $\boldsymbol{F}_{BT2}$, $\boldsymbol{F}_1$, $\boldsymbol{F}_2$, $\boldsymbol{F}_3$

$\boldsymbol{\Phi}(\theta) \triangleq \begin{bmatrix} \cos\theta & -\sin\theta \\ \sin\theta & \mathrm{con}\theta \end{bmatrix}$ $\triangleq$: definition symbol

References

(1) Hagimoto, K. et al., An Analytical Study of the Kinematics of a Scroll Compressor, Mitsubishi Heavy Industries Technical Review, Vol.23 No.3 (1986) p.154

(2) Hirano, T. et al., Development of High Efficiency Scroll Compressors for Air Conditioners, Mitsubishi Heavy Industries Technical Review, Vol.26 No.3 (1989) p.166

(3) Hirano, T. et al., Measurement of Scroll Compressor Driving-Pin Strain for Heat Pump, Processing of 25th Air-Conditioning and Refrigeration Conference, (1991) p.69

(4) Kasuga, H. et al., Measurement of Load Distribution in Four-Row Taperd Roller Bearings Installed in "Work Roll Shift" Rolling Mills, NSK Technical J., No.649 (1988) p.19

(5) Hirano, T. et al., Scroll Profiles for Fluid Machines, Mitsubishi Heavy Industries Technical Review, Vol.27 No.1 (1990) p.35